

NUCLEAR BASED TECHNIQUES FOR PROTON THERAPY MONITORING*

S. Aldawood, J. Bortfeldt, B. Gerling, C. Lang, R. Lutter, M. März, B. Tegetmeyer,
K. Parodi, P.G. Thirolf, LMU Munich
H. v.d. Kolff, LMU Munich / TU Delft
M. Böhmer, R. Gernhäuser, L. Maier, TU Munich

DEVELOPMENT OF A COMPTON CAMERA

Online ion beam range verification is one of the key issues in hadron therapy on the way to fully exploit its advantages by reliably monitoring the dose delivery. As a milestone on this way, we are developing and characterizing a Compton Camera prototype, aiming at the detection of prompt γ rays from the interaction of proton or ion beams with the target material. In particular, we will use this detector to monitor the laser-accelerated proton beams developed at CALA within the MAP Excellence Cluster. Our prototype consists of a scatter detector (a stack of 6 double-sided Si-strip detectors, $50 \times 50 \text{ mm}^2$, 0.5 mm thick, each 2×128 segments, read out by a highly integrated, ASIC-based electronics) and an absorber (a LaBr_3 scintillation crystal, $50 \times 50 \times 30 \text{ mm}^3$, read out by multi-anode photomultiplier, presently providing 64 channels of $6 \times \text{mm}^2$ pixel size). This detector system exploits the Compton scattering kinematics for the position reconstruction of a γ source. The layered structure of the scatter detectors allows for additional tracking of the Compton electrons and thus for an increased reconstruction efficiency. Fig. 1 shows the different components of the Compton camera (left: LaBr_3 scintillator, right: stack of double-sided silicon strip detectors with readout electronics).

Extensive simulations with the MEGlib simulation and image reconstruction code [1] predict an angular resolution of about 2° at 5 MeV photon energy (corresponding to ca. 2 mm spatial resolution for a source-target distance of 50 mm, as it is typical for a small-animal irradiation scenario). In laboratory characterization tests the performance of the LaBr_3 scintillator was determined both for an absorptive and a reflective finish of the side surfaces. The reflective coating resulted in a significantly improved performance, both for the energy resolution ($\Delta E/E = 3.9\%$ at 662 keV, compared to 12.5% for the absorptive coating) as well as for the time resolution (270 ps vs 543 ps, respectively). The point spread function has been determined with a collimated ^{137}Cs source (1 mm diameter), sequentially irradiating each pixel. A second position measurement campaign is in progress with 0.5 mm stepsize and collimation, aiming at creating a light distribution data base as required for an algorithm ('k-nearest neighbor') to reconstruct the centroid

of the primary photon interaction developed by the Delft group [2]. Hereby we aim at deriving the point spread function with a position resolution in the mm range. In addition, the integration of the scatter and absorber component of the Compton camera is ongoing, together with an upgrade of the readout electronics to fully exploit the 256-fold segmentation of the PMT. In a first beamtime at the Garching Tandem accelerator ($E_p = 20 \text{ MeV}$) a water phantom was irradiated and first operational experience on counting rates, noise sensitivity and background components was gained using the full Compton camera setup, which was operated using a precursor version of the silicon detectors, where only one side could be used for position analysis. In the meanwhile, the final set of detectors has been delivered by the manufacturer.

Moreover, an arrangement of 3-4 Compton camera modules could be used to extend the scope of medically usable PET isotopes to the class of $\beta^+\gamma$ -emitting species, which so far have been excluded from medical application due to the resulting extra dose delivered to the patient, as well as the expected increase of background from Compton scattering or even pair creation. However, provided the availability of customized gamma cameras, this alleged disadvantage could be turned into a promising benefit, offering a higher sensitivity for the reconstruction of the radioactivity distribution in PET examinations. Determining the intersection of the Compton cone derived from the third prompt photon emitted from the β^+ -daughter isotope with the line-of-response (LOR) as defined by the positron annihilation allows for a sensitive reconstruction of the decay position of the PET isotope [3].

Finally, the Compton camera would also provide the opportunity for building a 'hybrid detector', where during hadron-therapy treatment prompt photons could be detected from nuclear reactions of the therapeutic proton or ion beam with the tissue, while in the treatment interrupts delayed emission of photons from $\beta^+(\gamma)$ decay of online produced β^+ emitters ($^{10,11}\text{C}$, $^{14,15}\text{O}$) could be detected.

PRODUCTION CROSS SECTION OF β^+ EMITTERS RELEVANT FOR HADRON THERAPY

Production cross sections of β^+ -decaying isotopes from proton-induced nuclear reactions are important ingredients to treatment planning simulations in hadron therapy, which in some cases still lack the desired accuracy of about 5%.

* Work supported by the DFG Cluster of Excellence Munich-Centre for Advanced Photonics (MAP)

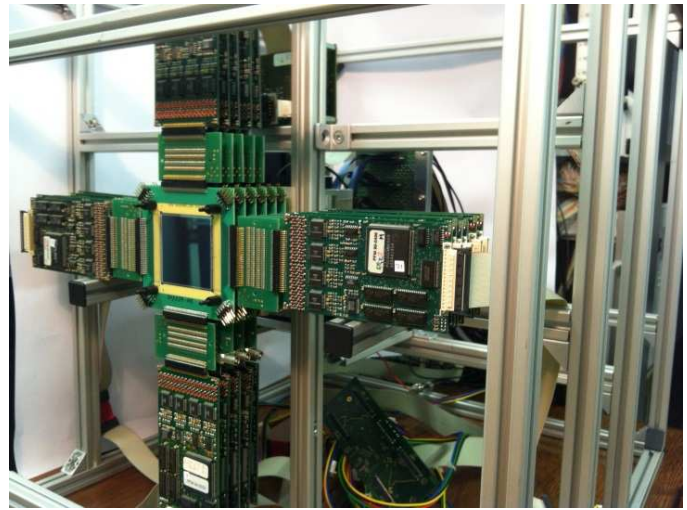
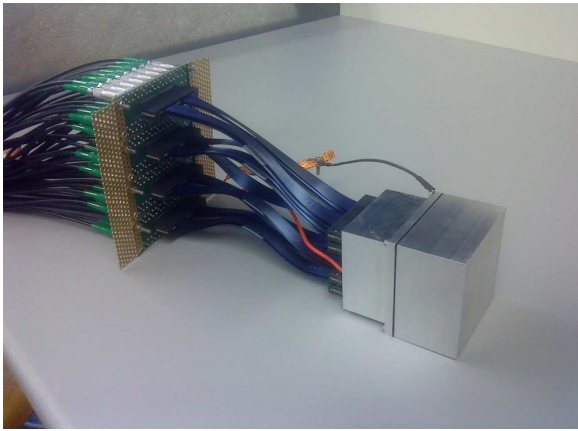


Figure 1: Left: LaBr₃ absorber crystal of the Compton camera, read out by a multi-anode PMT. Right: Scatter component of the Compton camera, consisting of a stack of 6 double-sided silicon strip detectors, read out via an ASIC-based integrated electronics.

We have started a measurement campaign to develop the methodology to improve the accuracy of β^+ emitters relevant for hadron therapy (^{13}N , $^{10,11}\text{C}$, $^{14,15}\text{O}$), starting with the cross section for ^{13}N via the reaction $^{16}\text{O}(p,\alpha)^{13}\text{N}$ at $E_p = 7 - 18$ MeV, due to the low reaction threshold that allows for measurements using the proton beam from the MLL Tandem accelerator. Fig. 2 displays the excitation function of ^{13}N as reported in [4].

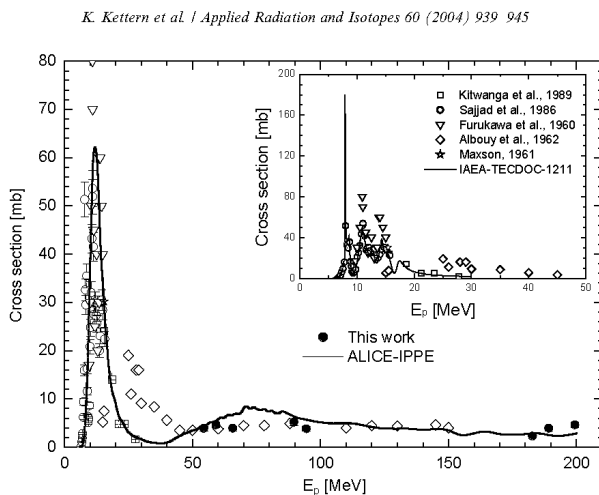


Figure 2: Excitation function of ^{13}N according to [4].

We used SiO₂ targets for an activation measurement. The target was irradiated for 15 minutes with a proton beam of 50-100 nA, then removed from the target chamber and transported to a shielded setup of 2 closely-spaced NaI detectors. Following conversion in 2 mm Cu plates, the 511 keV annihilation radiation is detected in coincidence. Counting rates at the start of the decay measurement amounted to about 1-2 kHz, resulting in a (starting

deadtime of about 30%). Besides the energy spectra, the time-dependent decay curve of the activated reaction products is measured via a time stamping provided by the VME QDC modules, while the (time-dependent) dead-time correction of the DAQ system is derived from a scaler that is read out every second. In order to monitor potential beam current fluctuations as well as the quality of the beam focusing, a (5 mm thick) Si detector is located at backward angles (135°) in the scattering chamber to measure the RBS amplitude. In addition, a charge integrator connected to the Faraday cup behind the target is read out every second. First measurements emphasized the necessity of an optimized beam focus at the target position in order to avoid activation of target holder components that may distort the ^{13}N decay curve. Therefore an improved setup contains a quartz monitor mounted on the target ladder, viewed by a camera through a viewport. Moreover, the target frame is shielded from direct view to the impinging beam by a (1mm thick) Ta aperture, a similar shield turned out to be necessary at the rear side of the target to prevent activation from protons backscattered from the Faraday cup. Finally, the target will be removed from the ladder and placed between the Cu converter plates for the decay measurement, thus reducing the amount of material exposed to the activating beam and brought close to the photon counters. These precautions turned out to be essential to allow for a reliable measurement of the desired ^{13}N decay curve and as such for the targeted accurate determination of the corresponding production cross section.

REFERENCES

- [1] A. Zoglauer et al., *New Astron. Rev.* 50 (2006) 629.
- [2] H.T. van Dam et al., *IEEE Trans. Nucl. Sci.* 58 (2011) 2139.
- [3] C. Lang et al., *Journal of Instrumentation* 9 (2014) P01008.
- [4] K. Ketterm et al., *Appl. Rad. Isotop.* 60 (2004) 939.